SEMARAK ILMU PUBLISHING

Journal of Advanced Research in Fluid Mechanics and Thermal Sciences

Journal homepage:
https://semarakilmu.com.my/journals/index.php/fluid_mechanics_thermal_sciences/index
ISSN: 2289-7879

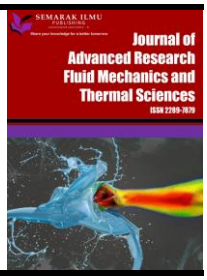

Stability Analysis of Unsteady Flow and Heat Transfer of Rear Stagnation Point in Hybrid Nanofluids with Thermal Radiation and Magnetic Impact

Nurul Amira Zainal[1,2,*], Iskandar Waini[2,3], Najiyah Safwa Khashi'ie[1,2], Khairum Hamzah[2,3], Sayed Kushairi Sayed Nordin[1,2], Abdul Rahman Mohd Kasim[4], Roslinda Nazar[5], Ioan Pop[6]

[1] Fakulti Teknologi dan Kejuruteraan Mekanikal, Universiti Teknikal Malaysia Melaka, 76100 Durian Tunggal, Melaka, Malaysia
[2] Forecasting and Engineering Technology Analysis (FETA) Research Group, Universiti Teknikal Malaysia Melaka, 76100 Durian Tunggal, Melaka, Malaysia
[3] Fakulti Teknologi dan Kejuruteraan Industri dan Pembuatan, Universiti Teknikal Malaysia Melaka, 76100 Durian Tunggal, Melaka, Malaysia
[4] Pusat Sains Matematik, Universiti Malaysia Pahang, Lebuhraya Persiaran Tun Khalil Yaakob, 26300 Kuantan, Pahang, Malaysia
[5] Department of Mathematical Sciences, Faculty of Science and Technology, Universiti Kebangsaan Malaysia, 43600 Bangi, Selangor, Malaysia
[6] Department of Mathematics, Babes-Bolyai University, Cluj-Napoca, Romania

ARTICLE INFO

Article history:
Received 25 August 2023
Received in revised form 16 November 2023
Accepted 23 November 2023
Available online 15 December 2023

Keywords:
Stability analysis; hybrid nanofluids; unsteady flow; thermal radiation; MHD

ABSTRACT

In this study, the stability analysis is conducted in order to observe the reliability of the generated solutions. The influence of several parameters is taken into consideration including magnetic parameter, radiation parameter, and heat transfer. The well-known heat transfer fluid that is Al_2O_3-Cu/H_2O hybrid nanofluid past a rear stagnation point is implied. The similarity equations are achieved after implying suitable similarity transformation which then needed to be solved numerically using bcp4c, embedded in MATLAB software. Dual solutions are observed along the investigation within specified values of involved parameters. It is important to note that verification results show excellent concordance with pre-existing reports.

1. Introduction

Recently, hybrid nanofluids have been developed to improve the thermophysical and heat-transfer properties. But choosing the right nanoparticles is important in stabilising the composition of hybrid nanofluid. Therefore, further research is needed to fully exploit the potential of this potent nanofluid mixture. The effectiveness of hybrid nanofluids as heat-transfer fluids in a range of flows and surfaces has recently been the subject of numerous investigations. One of the important areas that are crucial in investigating fluid flow is stagnation flow. Due to its significance in the field of engineering, the stagnation flow has drawn the attention of scholars. Greco *et al.,* [1] analyzed the flow control over the rear stagnation point and concluded that the first flow manipulation technique of the contemporary age may be the control of a flow through the suction of the boundary layer.

* *Corresponding author.*
E-mail address: nurulamira@utem.edu.my

https://doi.org/10.37934/arfmts.112.1.8493

However, the previously cited studies are focused on steady flows. It is possible for the flow to become unstable in some circumstances due to a change in the surface temperature and the free stream velocity. Devi *et al.,* [2] utilised boundary layer assumptions to examine how the buoyancy factor may affect the unsteady flow. Fang and Jing [3] discovered the exact solutions in the unsteady rear stagnation point flow. The analytical and numerical study of the heat transfer and boundary layer flow in the unsteady flow of nanofluid may be obtained in Saidin *et al.,* [4], Fathinia and Hussein [5], Yahaya *et al.,* [6], and Xu *et al.,* [7].

The current work is concerned with filling a knowledge gap, notably in the area of unsteady rear stagnation point flow with the effects of thermal radiation in a hybrid nanofluid. The main contribution of this study is the formulation of a new mathematical hybrid nanofluids model with the inclusion of the thermal radiation parameter, which also witnessed the appearance of several other significant variables like the suction and unsteady effect. This study also noted the establishment of numerous solutions. Given the considerable relevance practical of the boundary layer flow, this important discovery could contribute to a better knowledge of this research. This study also remarked on the appearance of multiple solutions.

2. Methodology

The unsteady magnetohydrodynamics (MHD) rear stagnation-point flow in hybrid nanofluids with radiation impact is studied as depicted in Figure 1.

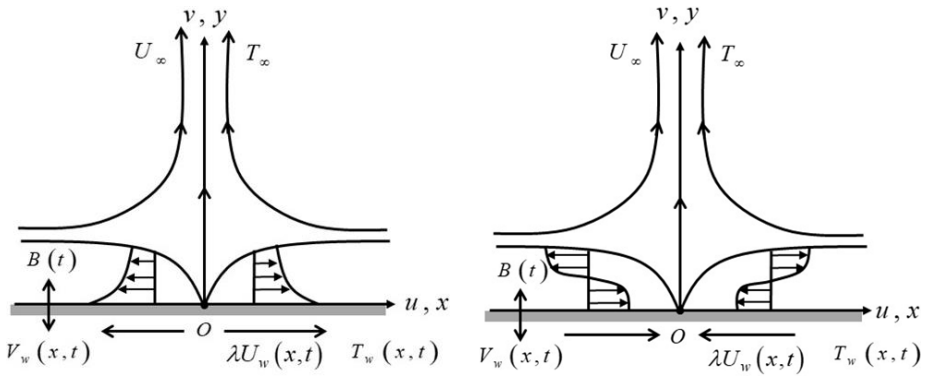

Fig. 1. The coordinate systems for (a) stretching (b) shrinking sheet

It is noted that $u_\infty = -u_0 x/(1-\xi t)$, is velocity of free stream where u_0 and ξ are constants that calculate the unsteadiness strength. The moving velocity is $u_w = u_0 x/(1-\xi t)$, the velocity and temperature towards wall transpiration is $v_w(x,t)$ and $T_w(x,t) = T_\infty + T_0 x/L(1-\xi t)$, respectively, whilst T_∞ is a surrounding temperature. Based on the above assumption, the governing equations of the hybrid nanofluids mathematical model can be written as [2,3]:

$$\frac{\partial u}{\partial x} + \frac{\partial v}{\partial y} = 0, \tag{1}$$

$$\frac{\partial u}{\partial t} + u\frac{\partial u}{\partial x} + v\frac{\partial u}{\partial y} = \frac{\partial u_\infty}{\partial t} + u_\infty \frac{\partial u_\infty}{\partial x} + \frac{\mu_{hnf}}{\rho_{hnf}}\frac{\partial^2 u}{\partial y^2} - \frac{\sigma_{hnf}}{\rho_{hnf}} B_0^2 (u - u_\infty), \tag{2}$$

$$\frac{\partial T}{\partial t}+u\frac{\partial T}{\partial x}+v\frac{\partial T}{\partial y}=\frac{k_{hnf}}{\left(\rho C_p\right)_{hnf}}\frac{\partial^2 T}{\partial y^2}-\frac{1}{\left(\rho C_p\right)_{hnf}}\frac{\partial q_r}{\partial y}. \tag{3}$$

Next, using the Rosseland approximation, the radiative heat flux q_r is given by [8]:

$$q_r=-\frac{4\sigma^*}{3k^*}\frac{\partial T^4}{\partial y}, \tag{4}$$

where k^* is the mean absorption coefficient and σ^* is the Stefan-Boltzman constant. Now, assume that temperature difference within the flow is such that T^4 may be expanded in Taylor's series. Thus, expanding T^4 about T_∞ and neglecting the higher-order terms we get

$$T^4\cong 4T_\infty{}^3T-3T_\infty{}^4, \tag{5}$$

hence,

$$\frac{\partial q_r}{\partial y}=-\frac{16T_\infty{}^3\sigma^*}{3k^*}\frac{\partial^2 T}{\partial y^2}. \tag{6}$$

Using Eq. (6) in Eq. (3) we obtain

$$\frac{\partial T}{\partial t}+u\frac{\partial T}{\partial x}+v\frac{\partial T}{\partial y}=\frac{k_{hnf}}{\left(\rho C_p\right)_{hnf}}\frac{\partial^2 T}{\partial y^2}+\frac{16T_\infty{}^3\sigma^*}{3k^*\left(\rho C_p\right)_{hnf}}\frac{\partial^2 T}{\partial y^2}. \tag{7}$$

Meanwhile, the boundary conditions of the above mathematical assumption are given as follows

$$\begin{aligned} &v=v_w\left(x,t\right),u=\lambda u_w\left(x,t\right),T=T_w\left(x,t\right),\quad \text{at } y=0,\\ &u\to u_\infty\left(x,t\right),T\to T_\infty\left(x\right),\quad \text{as } y\to\infty. \end{aligned} \tag{8}$$

The transverse magnetic field is denoted as B_0. Next, the thermophysical characteristic and correlation coefficient of related fluids are portrayed in Table 1 and Table 2, respectively.

Table 1
Properties of the base fluid and nanoparticles [9]

Component	$\rho(\mathrm{kg/m^3})$	$k(W/mK)$	C_p (J/kgK)
Al_2O_3	3970	40	765
H_2O	0.613	21	4179
Cu	8933	400	385

Table 2
Nanofluids with hybrid thermal properties [10,11]

Thermophysical properties	Alumina-Copper/Water (Al_2O_3–Cu/H_2O)
Thermal conductivity, k_{hnf}	$\frac{k_{hnf}}{k_f}=\left[\frac{\left(\frac{\phi_1 k_{Al_2O_3}+\phi_2 k_{Cu}}{\phi_{hnf}}\right)+2k_f+2\left(\phi_1 k_{Al_2O_3}+\phi_2 k_{Cu}\right)-2\phi_{hnf}k_f}{\left(\frac{\phi_1 k_{Al_2O_3}+\phi_2 k_{Cu}}{\phi_{hnf}}\right)+2k_f-\left(\phi_1 k_{Al_2O_3}+\phi_2 k_{Cu}\right)+\phi_{hnf}k_f}\right]$
Heat capacity, $\left(\rho C_p\right)_{hnf}$	$\left(\rho C_p\right)_{hnf}-\left(1-\phi_{hnf}\right)\left(\rho C_p\right)_f=\phi_1\left(\rho C_p\right)_{Al_2O_3}+\phi_2\left(\rho C_p\right)_{Cu}$
Electrical conductivity, σ_{hnf}	$\frac{\sigma_{hnf}}{\sigma_f}=\left[\frac{\left(\frac{\phi_1 \sigma_{Al_2O_3}+\phi_2 \sigma_{Cu}}{\phi_{hnf}}\right)+2\sigma_f+2\left(\phi_1 \sigma_{Al_2O_3}+\phi_2 \sigma_{Cu}\right)-2\phi_{hnf}\sigma_f}{\left(\frac{\phi_1 \sigma_{Al_2O_3}+\phi_2 \sigma_{Cu}}{\phi_{hnf}}\right)+2\sigma_f-\left(\phi_1 \sigma_{Al_2O_3}+\phi_2 \sigma_{Cu}\right)+\phi_{hnf}\sigma_f}\right]$

The following similarity variables is now presented as [3]

$$\psi\left(x,y,t\right)=\sqrt{\frac{u_0\nu_f}{\left(1-\xi t\right)}}xf\left(\eta\right),\ \eta=\sqrt{\frac{u_0}{\left(1-\xi t\right)\nu_f}}y,\ \theta\left(\eta\right)=\frac{T-T_\infty}{T_w-T_\infty}, \tag{9}$$

thus,

$$u=\frac{u_0 xf'\left(\eta\right)}{\left(1-\xi t\right)},\ v=-\sqrt{\frac{u_0\nu_f}{\left(1-\xi t\right)}}f\left(\eta\right),\ v_w=-\sqrt{\frac{u_0\nu_f}{\left(1-\xi t\right)}}S. \tag{10}$$

For further details, S in Eq. (10) is the parameter of mass flux and in this study, we only considered the positive values where $S>0$ which represents the suction parameter. The following ordinary (similarity) differential equations are then developed by utilising the similarity variables in Eq. (9) and Eq. (10) thus

$$\frac{\mu_{hnf}/\mu_f}{\rho_{hnf}/\rho_f}f'''+ff''-f'^2+1-\zeta\left(f'+\frac{\eta}{2}f''+1\right)-\frac{\sigma_{hnf}/\sigma_f}{\rho_{hnf}/\rho_f}M\left(f'+1\right)=0, \tag{11}$$

$$\frac{1}{\mathrm{Pr}}\left(\frac{1}{\left(\rho C_p\right)_{hnf}/\left(\rho C_p\right)_f}\right)\left(\frac{k_{hnf}}{k_f}+\frac{4}{3}Rd\right)\theta''+f\theta'-f'\theta-\zeta\left(\theta+\frac{\eta}{2}\theta'\right)=0, \tag{12}$$

$$\begin{aligned}&f\left(0\right)=S,\ f'\left(0\right)=\lambda,\ \theta\left(0\right)=1,\\&f'\left(\eta\right)\to-1,\ \theta\left(\eta\right)\to 0,\end{aligned} \tag{13}$$

where $M=\sigma_f B/u_0\,\rho_f$ represents MHD, $\mathrm{Pr}=\mu_f C_p/k_f$, and $\zeta=\xi/a$ signifies the unsteady characteristic. The radiation parameter is denoted as $Rd=4\sigma^*T_\infty^{\ 3}/k_f k^*$. The physical quantities related to this study is declared as

$$Nu_x = \frac{x}{k_f\left(T_w - T_\infty\right)}\left[-k_{hnf}\left(\frac{\partial T}{\partial y}\right)_{y=0} + \left(q_r\right)_{y=0}\right] \text{ and } C_f = \frac{\mu_{hnf}}{\rho_f u_\infty{}^2}\left(\frac{\partial u}{\partial y}\right)_{y=0}. \tag{14}$$

Then, we get

$$\mathrm{Re}_x^{1/2} C_f = \frac{\mu_{hnf}}{\mu_f} f''(0), \quad \mathrm{Re}_x^{-1/2} Nu_x = -\left(\frac{k_{hnf}}{k_f} + \frac{4}{3}Rd\right)\theta'(0), \tag{15}$$

where $\mathrm{Re}_x = u_0 x^2 / \nu_f\left(1-\xi t\right)$.

3. Stability Analysis

In this section, the stability analysis is conducted in order to verify the solution reliability since there is more than one solution in the obtained results. The following transformations are presented based on the work reported by Weidman *et al.,* [12], Harris *et al.,* [13] and Merkin [14]:

$$\begin{aligned} &u = \frac{u_0 x}{\left(1-\xi t\right)}\frac{\partial f}{\partial \eta}(\eta,\Phi),\ v = -\sqrt{\frac{u_0 \nu_f}{\left(1-\xi t\right)}} f\left(\eta,\Phi\right),\ \theta = \frac{T-T_\infty}{T_w - T_\infty}, \\ &\eta = y\sqrt{\frac{u_0}{\nu_f\left(1-\xi t\right)}},\ \Phi = u_0 t. \end{aligned} \tag{16}$$

By employing the new transformation in the above equation, now Eq. (7) to Eq. (9) are converting into

$$\frac{\mu_{hnf}/\mu_f}{\rho_{hnf}/\rho_f}\frac{\partial^3 f}{\partial \eta^3} + f\frac{\partial^2 f}{\partial \eta^2} - \left(\frac{\partial f}{\partial \eta}\right)^2 + \left(1-\xi\right)\left(\frac{\partial f}{\partial \eta} + \frac{\eta}{2}\frac{\partial^2 f}{\partial \eta^2} + 1\right) - \frac{\sigma_{hnf}/\sigma_f}{\rho_{hnf}/\rho_f} M\left(\frac{\partial f}{\partial \eta} + 1\right) - \frac{\partial^2 f}{\partial \eta \partial \Phi} = 0, \tag{17}$$

$$\frac{1}{\mathrm{Pr}}\left(\frac{1}{\left(\rho C_p\right)_{hnf}/\left(\rho C_p\right)_f}\right)\left(\frac{k_{hnf}}{k_f} + \frac{4}{3}Rd\right)\frac{\partial^2 \theta}{\partial \eta^2} + f\frac{\partial \theta}{\partial \eta} - \frac{\partial f}{\partial \eta}\theta - \xi\left(\theta + \frac{\eta}{2}\frac{\partial \theta}{\partial \eta}\right) - \frac{\partial \theta}{\partial \Phi} = 0, \tag{18}$$

$$\begin{aligned} &f\left(0,\Phi\right) = S,\ \frac{\partial f}{\partial \eta}(0,\Phi) = \lambda,\ \theta\left(0,\Phi\right) = 1, \\ &\frac{\partial f}{\partial \eta}(0,\Phi) \to 1,\ \theta\left(0,\Phi\right) \to 0,\ \text{as } \eta \to \infty. \end{aligned} \tag{19}$$

Next, we applied the perturbation functions described by Weidman *et al.,* [12], where it is given that

$$\begin{aligned} f\left(\eta,\Phi\right) &= f_0\left(\eta\right) + e^{-\Omega\Phi}\Upsilon\left(\eta,\Phi\right), \\ \theta\left(\eta,\Phi\right) &= \theta_0\left(\eta\right) + e^{-\Omega\Phi}\Lambda\left(\eta,\Phi\right), \end{aligned} \tag{20}$$

where $\Upsilon(\eta)$ and $\Lambda(\eta)$ are relatively small as compared with f_0, θ_0 and the unknown eigenvalue is assigned by Ω. Next, we substitute Eq. (16) into Eq. (17) and Eq. (18) which transformed the equations to the linear eigenvalue problem where

$$\frac{\mu_{hnf}/\mu_f}{\rho_{hnf}/\rho_f}\Upsilon''' + \left(f_0 - \xi\frac{\eta}{2}\right)\Upsilon'' - \left(2f_0' + \xi + \Omega + \frac{\sigma_{hnf}/\sigma_f}{\rho_{hnf}/\rho_f}M\right)\Upsilon' + f_0''\Upsilon = 0, \tag{21}$$

$$\frac{1}{\Pr}\left(\frac{1}{\left(\rho C_p\right)_{hnf}/\left(\rho C_p\right)_f}\right)\left(\frac{k_{hnf}}{k_f} + \frac{4}{3}Rd\right)\Lambda'' + \left(f_0 - \xi\frac{\eta}{2}\right)\Lambda' - \left(f_0' + \xi - \Omega\right)\Lambda - \theta_0\Upsilon' + \theta_0'\Upsilon = 0, \tag{22}$$

$$\begin{aligned}&\Upsilon(0) = 0,\ \Upsilon'(0) = 0,\ \Lambda(0) = 0,\\ &\Upsilon'(0) \to 1,\ \Lambda(0) \to 0,\ \text{as } \eta \to \infty.\end{aligned} \tag{23}$$

Without losing generality, we fix the value of $\Upsilon''(0)$ as $\Upsilon''(0) = 1$ in the current study and derive the value of Ω from the system of equations in (21) and (22) in addition to the boundary condition (23). According to Eq. (16), as time passes, the flow is in a stable state if Ω is positive and for negative values of Ω, the flow is said to be in a state of instability. Meanwhile, when Ω approaches the critical value or bifurcation point, the values of Ω tend to zero for both positive and negative sides.

4. Results Interpretations

In this section, the results obtained is discussed thoroughly. The results validations are examined with Bhattacharyya [15] and Turkyilmazoglu *et al.,* [16] (see Table 3). It is found that the present discoveries are very much in line with previous investigations. As a result, we are confident that the intended computer model can accurately anticipate the behaviour of dynamic fluid flow. In this study, a variety of ϕ is implemented i.e., $0.00 \le \phi_1, \phi_2 \le 0.01$. Furthermore, a variety of controlling parameter values are defined to the preceding scope where the value of the magnetic and unsteadiness parameter is fixed to $M = 6.0,\ \zeta = -2.0$, while the suction and radiation parameter are set within $4.0 \le S \le 5.0$ and $0.0 \le Rd \le 0.5$, respectively. It should be emphasised that, in order to achieve the desired result, the values of the supplied parameter should be utilised to generate an adequate result estimation.

Table 3
Results generation of $\mathrm{Re}_x^{1/2} C_f$ with various λ when $\varepsilon = M = \delta = S = \phi_1 = \phi_2 = 0$

λ	Present result		Bhattacharyya [15]		Turkyilmazoglu *et al.,* [16]	
	FS	SS	FS	SS	FS	SS
−1.00	1.3288169	0.0000000	1.3288169	0.0000000	1.3288168	0.0000000
−1.15	1.0822312	0.1167021	1.0822316	0.1167023	1.0822312	0.1167021
−1.20	0.9324733	0.2336497	0.9324728	0.2336491	0.9324733	0.2336497
−1.2465	0.5842817	0.5542962	0.5842915	0.5542856	0.5842813	0.5542947
−1.24657	0.5745257	0.5640125	0.5745268	0.5639987	0.5774525	0.5640081

Figure 2 describes the influence of suction parameter S as the sheet shrinks. The improvement in velocity profiles $f'(\eta)$ in the first solution (FS) is displayed when the value of S improves over the shrinking sheet, as illustrated in Figure 2(a). Meanwhile, the trend of the temperature distributions profile $\theta(\eta)$ corresponds to the increment of S is accessible in Figure 2(b). In Figure 2(b), both solutions show a downward trend of $\theta(\eta)$ as hybrid nanofluid is endorsed. Overall, both velocity and temperature distribution profiles met the far-field boundary conditions (13) asymptotically when $\eta_\infty = 6$ is implemented.

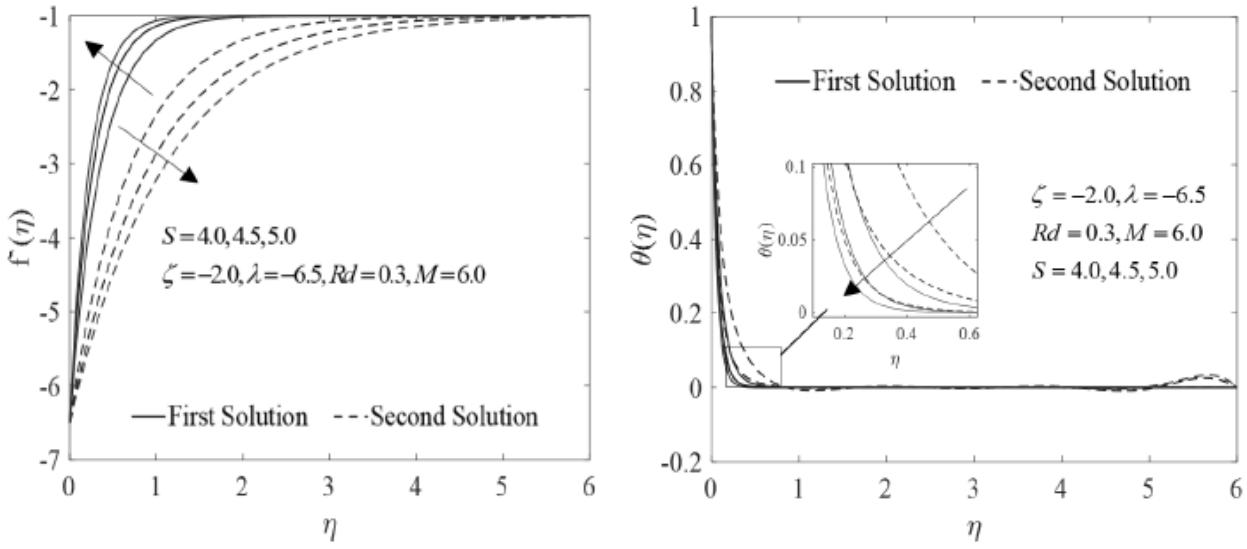

(a) (b)

Fig. 2. Distribution profiles with different S in contrast to η (a) velocity and (b) temperature profile

Figure 3(a) and Figure 3(b) depict the characteristics of $f'(\eta)$ and $\theta(\eta)$ with respect to the addition of magnetic parameter, M. Figure 3(a) apparently showed that the increasing values of M specifically in Al_2O_3-Cu/H_2O, lessen the thickness of boundary layer in the FS. However, the second solution (SS) showed the reduction trend as M increases. Meanwhile, it is observed that $\theta(\eta)$ presents a downward trend in both solutions, as exhibited in Figure 3(b). As can be seen, the characteristics of temperature distribution profile which also remark the thermal boundary layer thickness declines in both solutions. The effect of unsteadiness parameter ζ are portrayed in Figs. 4(a) and 4(b) concerning $f'(\eta)$ and $\theta(\eta)$, respectively. Figure 4(a) displays that as ζ improved, $f'(\eta)$ decrease in the FS, while the alternative solutions point out the opposite. On the other hand, Figure 4(b) illustrates a decreasing pattern of $\theta(\eta)$ when ζ improves in FS and SS, hence we can conclude that the thermal performance has progressed as ζ enhances and also decreased the thickness of the boundary layer.

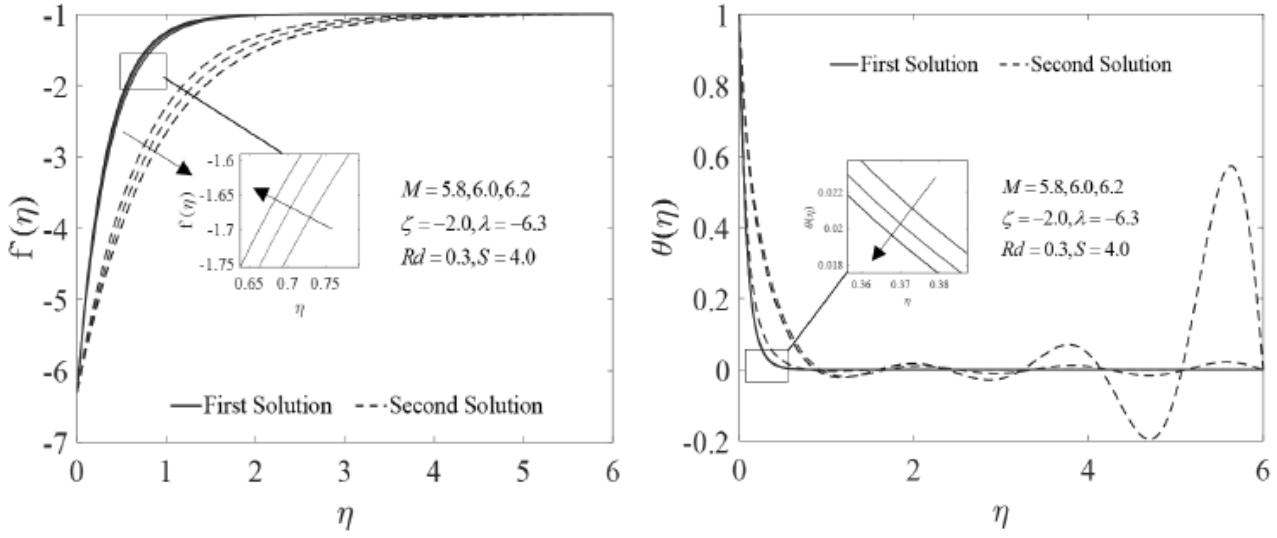

(a) (b)

Fig. 3. Distribution profiles with different M in contrast to η (a) velocity profile (b) temperature profile

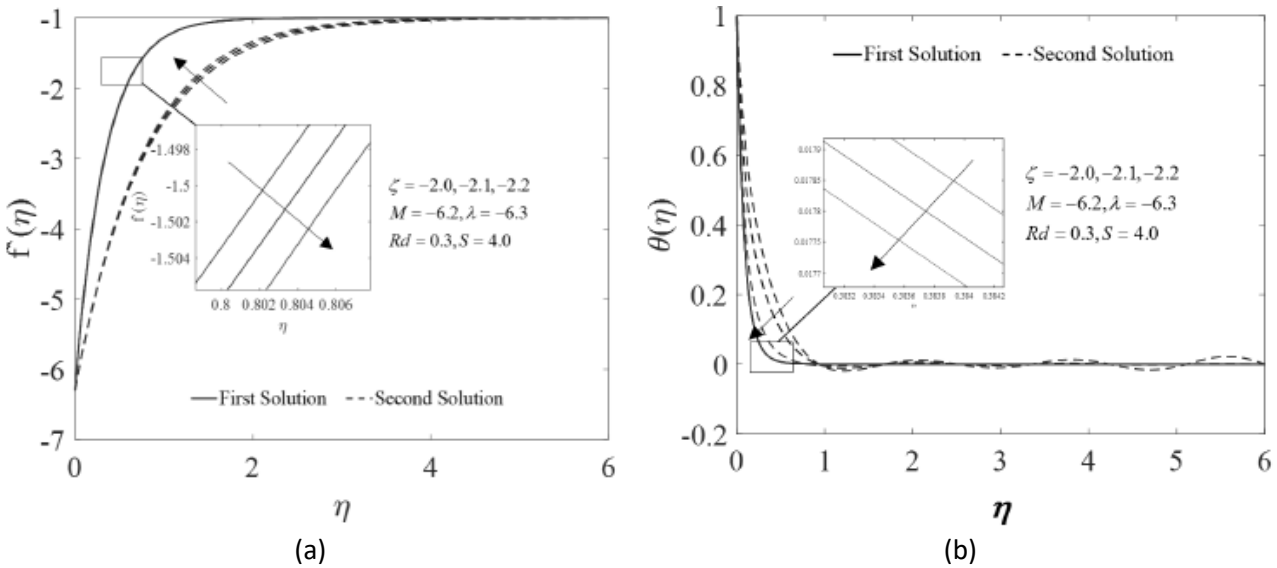

(a) (b)

Fig. 4. Distribution profiles with different ζ in contrast to η (a) velocity profile (b) temperature profile

Figure 5 illustrates the dimensionless temperature profile $\theta(\eta)$ in relation to the thermal radiation parameter *Rd*. It has been observed that *Rd* exerts a discernible influence on the temperature of hybrid nanofluids. This phenomenon is primarily due to the conversion of thermal energy, resulting in a thicker thermal boundary layer. Additionally, it can be attributed to the increased generation and release of heat into the flow, resulting in the augmentation of the boundary layer thickness due to the presence of radiation components. Consequently, this also indicating a higher rate of energy transfer to the hybrid nanofluids, which leads to an elevation in the temperature of the hybrid nanofluids. Figure 6 demonstrates the results of stability analysis to test the reliability of the solutions. When $e^{-\Omega}\Phi \to 0$ as $\Phi \to \infty$, it is recorded that Ω generates positive eigenvalues. Meanwhile, $e^{-\Omega}\Phi \to \infty$ is recorded to be negative eigenvalues. These findings suggest that the FS is long-term stable, whereas the SS is unstable and therefore not long-term physically dependable.

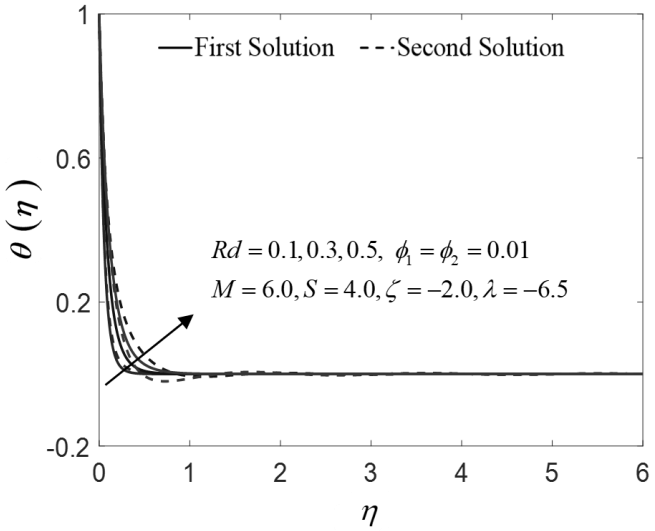

Fig. 5. Different values of Rd for temperature profile

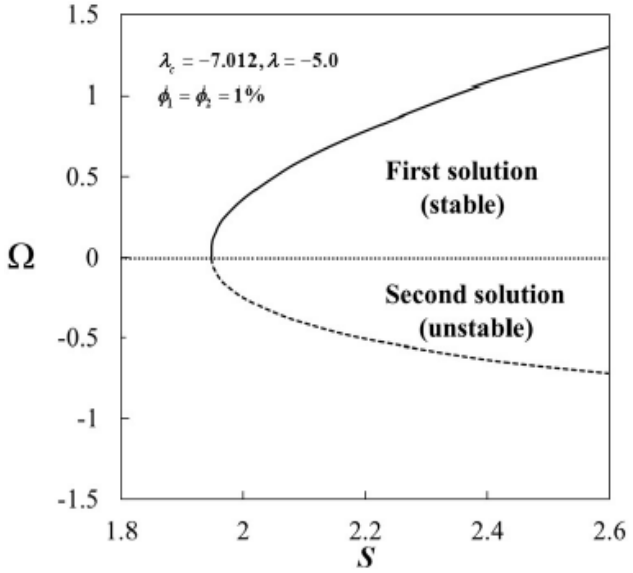

Fig. 6. Smallest eigenvalue for various S

5. Conclusions

The recent study verified a numerical simulation of Al_2O_3-Cu/H_2O hybrid nanofluid's response to several impact along a shrinking sheet in unsteady rear stagnation point flow. The results of increasing suction and magnetic parameter driven the decrement of boundary layer thickness. Meanwhile, the enhancement of unsteadiness parameter leads to increment of boundary layer thickness. Through the stability analysis, the FS has been demonstrated to be in a stable state, while the SS responds the opposite way.

Acknowledgement
The authors would like to acknowledge Universiti Teknikal Malaysia Melaka (UTeM) for the financial and technical support under the *Geran Insentif Penerbitan Jurnal 2020* (JURNAL/2020/FTKMP/Q00051).

References

[1] Greco, Carlo Salvatore, Gerardo Paolillo, Tommaso Astarita, and Gennaro Cardone. "The von Kármán street behind a circular cylinder: Flow control through synthetic jet placed at the rear stagnation point." *Journal of Fluid Mechanics* 901 (2020): A39. https://doi.org/10.1017/jfm.2020.427

[2] Devi, C. D. Surma, H. S. Takhar, and G. Nath. "Unsteady mixed convection flow in stagnation region adjacent to a vertical surface." *Wärme-und Stoffübertragung* 26, no. 2 (1991): 71-79. https://doi.org/10.1007/BF01590239

[3] Fang, Tiegang, and Wei Jing. "Closed-form analytical solutions of flow and heat transfer for an unsteady rear stagnation-point flow." *International Journal of Heat and Mass Transfer* 62 (2013): 55-62. https://doi.org/10.1016/j.ijheatmasstransfer.2013.02.049

[4] Saidin, Norshaza Atika, Mohd Ariff Admon, and Khairy Zaimi. "Unsteady Three-Dimensional Free Convection Flow Near the Stagnation Point Over a General Curved Isothermal Surface in a Nanofluid." *CFD Letters* 12, no. 6 (2020): 80-92. https://doi.org/10.37934/cfdl.12.6.8092

[5] Fathinia, F., and Ahmed Kadhim Hussein. "Effect of blockage shape on unsteady mixed convective nanofluid flow over backward facing step." *CFD Letters* 10, no. 1 (2018): 1-18.

[6] Yahaya, Rusya Iryanti, Norihan Md Arifin, Ioan Pop, Fadzilah Md Ali, and Siti Suzilliana Putri Mohamed Isa. "Dual Solutions of Unsteady Mixed Convection Hybrid Nanofluid Flow Past a Vertical Riga Plate with Radiation Effect." *Mathematics* 11, no. 1 (2023): 215. https://doi.org/10.3390/math11010215

[7] Xu, Xiangtian, Gaosheng Li, Yuqin Zhao, and Tiejun Liu. "Analytical solutions for heat conduction problems with three kinds of periodic boundary conditions and their applications." *Applied Mathematics and Computation* 442 (2023): 127735. https://doi.org/10.1016/j.amc.2022.127735

[8] Rosseland, Svein. *Theoretical Astrophysics: Atomic theory and the analysis of stellar atmospheres and envelopes*. Clarendon Press, 1936.

[9] Abu-Nada, Eiyad, and Hakan F. Oztop. "Effects of inclination angle on natural convection in enclosures filled with Cu-water nanofluid." *International Journal of Heat and Fluid Flow* 30, no. 4 (2009): 669-678. https://doi.org/10.1016/j.ijheatfluidflow.2009.02.001

[10] Takabi, Behrouz, and Saeed Salehi. "Augmentation of the heat transfer performance of a sinusoidal corrugated enclosure by employing hybrid nanofluid." *Advances in Mechanical Engineering* 6 (2014): 147059. https://doi.org/10.1155/2014/147059

[11] Ghalambaz, Mohammad, Natalia C. Roşca, Alin V. Roşca, and Ioan Pop. "Mixed convection and stability analysis of stagnation-point boundary layer flow and heat transfer of hybrid nanofluids over a vertical plate." *International Journal of Numerical Methods for Heat & Fluid Flow* 30, no. 7 (2020): 3737-3754. https://doi.org/10.1108/HFF-08-2019-0661

[12] Weidman, P. D., D. G. Kubitschek, and A. M. J. Davis. "The effect of transpiration on self-similar boundary layer flow over moving surfaces." *International Journal of Engineering Science* 44, no. 11-12 (2006): 730-737. https://doi.org/10.1016/j.ijengsci.2006.04.005

[13] Harris, S. D., D. B. Ingham, and I. Pop. "Mixed convection boundary-layer flow near the stagnation point on a vertical surface in a porous medium: Brinkman model with slip." *Transport in Porous Media* 77 (2009): 267-285. https://doi.org/10.1007/s11242-008-9309-6

[14] Merkin, J. H. "On dual solutions occurring in mixed convection in a porous medium." *Journal of Engineering Mathematics* 20, no. 2 (1986): 171-179. https://doi.org/10.1007/BF00042775

[15] Bhattacharyya, Krishnendu. "Dual solutions in boundary layer stagnation-point flow and mass transfer with chemical reaction past a stretching/shrinking sheet." *International Communications in Heat and Mass Transfer* 38, no. 7 (2011): 917-922. https://doi.org/10.1016/j.icheatmasstransfer.2011.04.020

[16] Turkyilmazoglu, Mustafa, Kohilavani Naganthran, and Ioan Pop. "Unsteady MHD rear stagnation-point flow over off-centred deformable surfaces." *International Journal of Numerical Methods for Heat & Fluid Flow* 27, no. 7 (2017): 1554-1570. https://doi.org/10.1108/HFF-04-2016-0160